APPLIED PHYSICS LETTERS **90**, 181907 (2007)

Atomic arrangement variations of [0001]-tilt grain boundaries in ZnO thin films grown on *p*-Si substrates due to thermal treatment

J. W. Shin and J. Y. Lee
Department of Materials Science and Engineering, Korea Advanced Institute of Science and Technology, Daejeon 305-701, Korea

Y. S. No, J. H. Jung, and T. W. Kim[a)]
Advanced Semiconductor Research Center, Division of Electronics and Computer Engineering, Hanyang University, 17 Haengdang-dong, Seongdong-gu, Seoul 133-791, Korea

W. K. Choi
Thin Film Material Research Center, Korea Institute of Science and Technology, Seoul 136-701, Korea

(Received 3 November 2006; accepted 28 March 2007; published online 30 April 2007)

The plane-view high-resolution transmission electron microscopy (HRTEM) images in ZnO thin films grown on *p*-Si substrates showed that $(10\bar{1}0)$ asymmetric grain boundaries with a periodic array of strain contrast features existed in a sparse columnar structure for as-grown ZnO thin films and that $(11\bar{2}0)$ asymmetric grain boundaries and $(85\bar{13}0)$ symmetric grain boundaries existed in a dense columnar structure for annealed ZnO thin films. The atomic arrangement variations of [0001]-tilt grain boundaries in ZnO thin films grown on Si substrates due to thermal treatment are described on the basis of the HRTEM results. © *2007 American Institute of Physics*.
[DOI: 10.1063/1.2732177]

The growth of ZnO materials has attracted much attention for both scientific and technological reasons.[1–3] The novel physical properties of ZnO thin films and their large exciton binding energies and excellent chemical stabilities[4,5] have stimulated their potential applications in optoelectronic devices, such as light-emitting diodes,[6] laser diodes,[7] and solar cells.[8] The fabrication of lasers utilizing ZnO thin films and operating at room temperature has been particularly interesting due to their applications in promising optoelectronic devices operating in the ultraviolet region of the spectrum.[9–11] ZnO/Si heterostructures have become particularly attractive because of the integration of optoelectronic devices due to the large exciton binding energy of the ZnO thin film and the cheapness and the large size of the Si substrate.[12] Since the optical properties of ZnO thin films grown on Si substrates are significantly affected by the microstructural properties related to the grain boundaries of the films, studies concerning the atomic structures of the grain boundaries in ZnO thin films are necessary for improving the efficiencies of optoelectronic devices. Theoretical works on the microstructural properties of [0001]-tilt boundaries in wurtzite structural materials have been extensively performed.[13–21] However, relatively little experimental work has been done on the atomic structure of [0001]-tilt grain boundaries of materials with a wurtzite structure, such as ZnO[22–24] and GaN[25], and studies concerning variations in the atomic arrangements of [0001]-tilt grain boundaries in ZnO thin films grown on Si substrates due to thermal treatment have not yet been performed. Such investigations of the grain boundary variations in ZnO thin films due to thermal treatment are very important for understanding the deterioration of optoelectronic devices fabricated utilizing these films.

This letter reports data for atomic arrangement variations of [0001]-tilt grain boundaries due to thermal treatment in ZnO thin films grown on *p*-Si substrates by using the radio-frequency magnetron sputtering method. Transmission electron microscopy (TEM) measurements were performed to investigate the microstructural properties of the as-grown and the annealed ZnO thin films. The atomic arrangement variations of [0001]-tilt ZnO gain boundaries due to thermal treatment are described on the basis of high-resolution TEM (HRTEM) images.

Polycrystalline stoichiometric ZnO with a purity of 99.999% was used as a source target material and was precleaned by repeated sublimation. The carrier concentration of the B-doped *p*-Si substrates with (100) orientations used in this experiment was 1×10^{15} cm^{-3}. The substrates were degreased in trichloroethylene (TCE), rinsed in de-ionized water, etched in a mixture of HF and H_2O (1:1) at room temperature for 5 min, and rinsed in TCE again. After the Si wafers had been cleaned chemically, they were mounted onto a susceptor in the growth chamber. After the chamber had been evacuated to 8×10^{-7} Torr, the deposition was done at a substrate temperature of 600 °C. Ar gas with a purity of 99.999% was used as the sputtering gas. Prior to ZnO growth, the surface of the ZnO target was polished by Ar^+ sputtering. The ZnO deposition was done at a system pressure of 0.021 Torr and a radio-frequency power (radio frequency=13.26 MHz) of 100 *W*. The flow-rate ratio of Ar to O_2 was 2, and the growth rate was approximately 1.17 nm/min.

The TEM measurements were performed using a JEM-ARM1300S transmission electron microscope operating at 1.25 MeV. The samples for the plane-view TEM measurements were prepared by cutting and polishing with diamond paper to a thickness of approximately 30 μm and then argon-ion milling at liquid-nitrogen temperature to electron transparency.

a)Author to whom correspondence should be addressed; electronic mail: twk@hanyang.ac.kr

 © 2007 American Institute of Physics
Downloaded 15 Apr 2011 to 143.248.103.56. Redistribution subject to AIP license or copyright; see http://apl.aip.org/about/rights_and_permissions

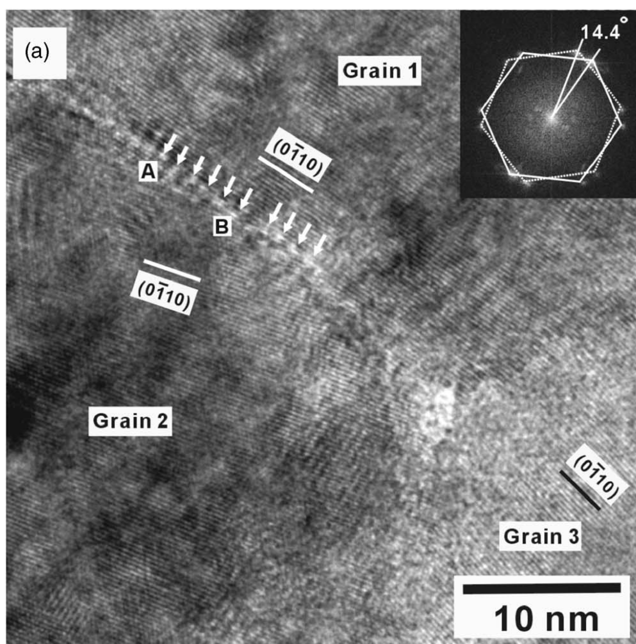

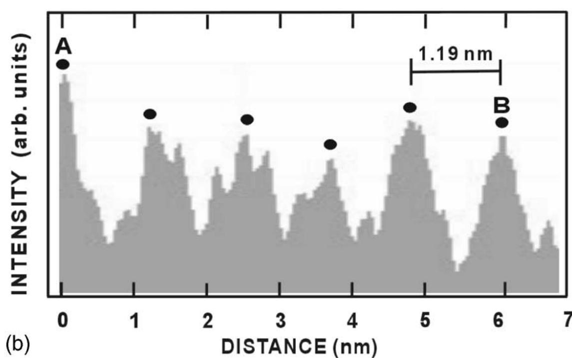

FIG. 1. (a) Plane-view high-resolution transmission electron microscopy image around a triple junction for an as-grown ZnO film grown on a *p*-Si (100) substrate. (b) Histogram obtained from A to B in (a) and indicating the magnitude of the strain contrast feature.

Figure 1(a) shows a plane-view HRTEM image around a triple junction in an as-grown ZnO thin film grown on a *p*-Si (100) substrate. Because the diffusion rate of the atoms on the as-grown ZnO surface during the growth of the columnar is smaller than their deposition rate, the atoms on the ZnO surface cannot occupy stable positions, resulting in the formation of the sparse columnar structures, as shown in Fig. 1(a). The grain boundaries between grains 1 and 3 and between grains 2 and 3 are not clearly observed due to the existence of the sparse columnar structures of the as-grown ZnO thin film. The rotation angle between grains 1 and 2, as determined from the fast Fourier transform of the HRTEM image shown in the inset of Fig. 1(a), is 14.4°. An asymmetric grain boundary with a rotation angle of 14.4° consisting of a periodic array of strain contrast features, which is the $(10\bar{1}0)$ plane of grain 1, is clearly observed. The histogram obtained by a line scan along the $(01\bar{1}0)$ plane of grain 1 from the position denoted by A to that denoted by B indicates that the strain contrast features are arrayed periodically with an average distance of 1.19 nm, as shown in Fig. 1(b).

A schematic diagram of the atomic arrangement of the asymmetric grain boundary with a rotation angle of 14.4°, viewed along the [0001] direction, is shown in Fig. 2. The small and the large circles denote Zn and O atoms, respectively.

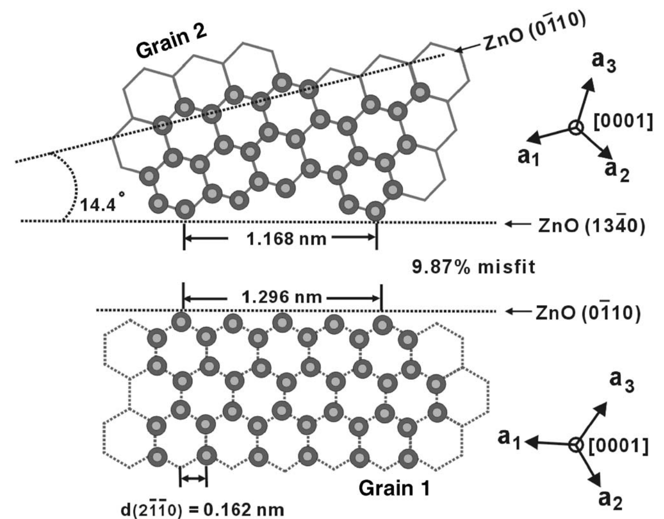

FIG. 2. Schematic diagram of the atomic arrangement of the asymmetric grain boundary with a rotation angle of 14.4° viewed along the [0001] direction in the ZnO thin film. The small and the large circles denote Zn and O atoms, respectively.

When grain 2 is tilted by 14.4°, the $(13\bar{4}0)$ plane of grain 2 is almost parallel to the $(0\bar{1}10)$ plane of grain 1. The angle between the $(13\bar{4}0)$ and the $(0\bar{1}10)$ planes, as determined from the theoretical equation,[26] is 13.9°, which is slightly different from the experimental value. Because the (*hki*0) plane in the wurtzite structure has a periodic atomic array with a finite distance, grain 2 has a periodic atomic array along the $(13\bar{4}0)$ plane with a theoretical distance of 1.168 nm. The theoretical distance of the periodic atomic array of 1.168 nm in grain 2 is consistent with that of 8 $\times d_{(2\bar{1}\bar{1}0)}$=1.296 nm in grain 1, where $d_{(2\bar{1}\bar{1}0)}$ is the distance between the $(2\bar{1}\bar{1}0)$ planes, as shown in Fig. 2. Because the misfit between the two grain boundaries is 0.0987, grain 1 is under a compressive stress in a direction parallel to the interface, and grain 2 is under a tensile stress in a direction parallel to the interface. Therefore, a periodic array of strain contrast features with an average spacing of approximately 1.2 nm is generated, which is in reasonable agreement with the experimental value of 1.19 nm.

Figure 3 shows a plane-view HRTEM image around a triple junction for an annealed ZnO thin film grown on a *p*-Si (100) substrate. The HRTEM image shows that the annealed ZnO thin film consists of dense columnar structures because the thermal energy is large enough to provide atomic mobility, resulting in atoms occupying stable positions. The rotation angles of the grain boundaries, as determined from the fast Fourier transform of the HRTEM image, are 19.7° and 15.1°. The asymmetric grain boundary with a rotation angle of 19.7° is composed of the $(11\bar{2}0)$ plane of grain 1, as indicated by the straight line and the $\{10\bar{1}0\}$ facet plane of grain 2, as indicated by the zigzag line. Three lower surface energy planes, (0001), $(11\bar{2}0)$, and $(01\bar{1}0)$, exist in the annealed ZnO thin films, and the corresponding energy densities are 0.099, 0.123, and 0.209 eV/Å^2.[27] The more stable grain boundaries in the [0001]-tilt grain boundary for the annealed ZnO film, which consist of the $\{11\bar{2}0\}$ and the $\{01\bar{1}0\}$ planes, might have been created during thermal annealing. However, even though the existence of the asym-

Downloaded 15 Apr 2011 to 143.248.103.56. Redistribution subject to AIP license or copyright; see http://apl.aip.org/about/rights_and_permissions

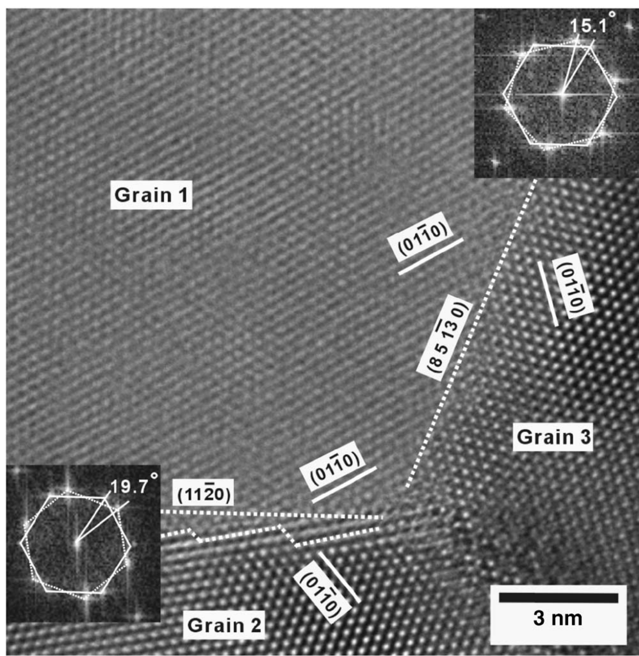

FIG. 3. Plane-view high-resolution transmission electron microscopy image around a triple junction for an annealed ZnO film grown on a *p*-Si (100) substrate.

metric tilt grain boundary forms a stable plane, since the asymmetric tilt grain boundary does not contain the most stable grain due to the existence of a distorted atomic structure, the asymmetric tilt grain boundary is metastable. A symmetric tilt grain boundary (STGB) with a rotation angle of 15.1° was observed between grains 1 and 3. Since the STGBs can be accommodated due to the misorientations resulting from the energy stabilization and the relaxation of the misfits existing between grains,[24] STGBs, which are the most stable grain boundaries, are generated during thermal annealing.

In summary, HRTEM images showed that sparse columnar structures with a $(0\bar{1}10)$ asymmetric grain boundary with a periodic array of strain contrast features existed in the as-grown ZnO thin film and that dense columnar structures with a $(11\bar{2}0)$ asymmetric grain boundary and a $(851\bar{3}0)$ symmetric grain boundary, which were more stable grain boundaries, existed in the annealed ZnO thin film. The atomic arrangement variations of the [0001]-tilt grain boundaries in the ZnO thin films due to thermal treatment were described on the basis of the HRTEM images. These results can help improve understanding of the thermal annealing effects on the microstructural properties of ZnO thin films grown on *p*-Si substrates.

This work was supported by the Korea Science and Engineering Foundation through the Quantum-functional Semiconductor Research Center at Dongguk University and by a grant (Code No. 06K1501-02510) from the Center for Nanostructured Materials Technology under 21st Century Frontier R&D Programs of the Ministry of Science and Technology, Korea. The authors would like to thank Youn-Joong Kim at the Korea Basic Science Institute for the use of high voltage electron microscopy transmission electron microscope.

[1] M. H. Huang, S. Mao, H. Feick, H. Q. Yan, Y. Y. Wu, H. Kind, E. Weber, R. Russo, and P. D. Yang, Science **292**, 1897 (2001).
[2] T. Makino, Y. Segawa, A. Tsukazaki, A. Ohtomo, and M. Kawasaki, Appl. Phys. Lett. **87**, 022101 (2005).
[3] Y. H. Tong, Y. C. Liu, C. L. Shao, and R. X. Mu, Appl. Phys. Lett. **88**, 123111 (2006).
[4] T. Aoki, Y. Hatanaka, and D. C. Look, Appl. Phys. Lett. **76**, 3257 (2000).
[5] R. F. Service, Science **276**, 895 (1997).
[6] W. Z. Xu, Z. Z. Ye, Y. J. Zeng, L. P. Zhu, B. H. Zhao, L. Jiang, J. G. Lu, and H. P. He, Appl. Phys. Lett. **88**, 173506 (2006).
[7] H. Kim, C. M. Gilmore, J. S. Jorwitz, A. Pigue, H. Murafa, G. P. Kushto, R. Schlaf, Z. H. Kafafi, and D. B. Chrisey, Appl. Phys. Lett. **76**, 259 (2000).
[8] U. Rau and M. Schmidt, Thin Solid Films **387**, 141 (2001).
[9] Z. K. Tang, G. K. L. Wong, P. Yu, M. Kawasaki, A. Ohtomo, H. Koinuma, and Y. Segawa, Appl. Phys. Lett. **72**, 3270 (1998).
[10] S. F. Yu, Clement Yuen, S. P. Lau, and H. W. Lee, Appl. Phys. Lett. **84**, 3244 (2004).
[11] H. D. Li, S. F. Yu, A. P. Abiyasa, Clement Yuen, S. P. Lau, H. Y. Yang, and Eunice S. P. Leong, Appl. Phys. Lett. **86**, 261111 (2005).
[12] K. Ogata, T. Kawanishi, K. Maejima, K. Sakurai, Sz. Fujita, and Sg. Fujita, J. Cryst. Growth **237**, 553 (2002).
[13] J. Chen, P. Ruterana, and G. Nouet, Phys. Rev. B **67**, 205210 (2003).
[14] A. Bere and A. Serra, Phys. Rev. B **66**, 085330 (2002).
[15] J. D. Rittner and D. N. Seidman, Phys. Rev. B **54**, 6999 (1996).
[16] M. Kohyama, Modell. Simul. Mater. Sci. Eng. **10**, R31 (2002).
[17] S. D. Mo, W. Y. Ching, M. F. Chisholm, and G. Duscher, Phys. Rev. B **60**, 2416 (1999).
[18] S. Fabris and C. Elsässer, Phys. Rev. B **64**, 245117 (2001).
[19] F. Oba, I. Tanaka, S. R. Nishitani, H. Adachi, B. Slater, and D. H. Gay, Philos. Mag. A **80**, 1567 (2000).
[20] F. Oba, S. R. Nishitani, H. Adachi, I. Tanaka, M. Kohyama, and S. Tanaka, Phys. Rev. B **63**, 045410 (2001).
[21] J. M. Carlsson, B. Hellsing, H. S. Domingos, and P. D. Bristowe, J. Phys.: Condens. Matter **13**, 9937 (2001).
[22] F. Oba, H. Ohta, Y. Sato, H. Hosono, T. Yamamoto, and Y. Ikuhara, Phys. Rev. B **70**, 125415 (2004).
[23] Y. Sato, T. Mizoguchi, F. Oba, M. Yodogawa, T. Yamamoto, and Y. Ikuhara, J. Mater. Sci. **40**, 3059 (2005).
[24] J. W. Shin, J. Y. Lee, Y. S. No, T. W. Kim, and W. K. Choi, Appl. Phys. Lett. **89**, 101904 (2006).
[25] V. Potin, P. Ruterana, G. Nouet, R. C. Pond, and H. Morkoç, Phys. Rev. B **61**, 5587 (2000).
[26] J. W. Edington, *Electron Diffraction in the Electron Microscope* (N. V. Philips' Gooeilampenfabrieken, Eindhoven, 1975), 1, p. 81.
[27] N. Fujimure, T. Nishifara, S. Goto, J. Xu, and T. Ito, J. Cryst. Growth **130**, 269 (1993).

Downloaded 15 Apr 2011 to 143.248.103.56. Redistribution subject to AIP license or copyright; see http://apl.aip.org/about/rights_and_permissions